

Lattice-Matched GaN–InAlN Waveguides at $\lambda = 1.55 \mu\text{m}$ Grown by Metal–Organic Vapor Phase Epitaxy

A. Lupu, F. H. Julien, S. Golka, G. Pozzovivo, G. Strasser, E. Baumann, F. Giorgetta, D. Hofstetter, S. Nicolay, M. Mosca, E. Feltin, J.-F. Carlin, and N. Grandjean

Abstract—We report on the demonstration of low-loss, single-mode GaN–InAlN ridge waveguides (WGs) at fiber-optics telecommunication wavelengths. The structure grown by metal–organic vapor phase epitaxy contains AlInN cladding layers lattice-matched to GaN. For slab-like WGs propagation losses are below 3 dB/mm and independent of light polarization. For 2.6- μm -wide WGs the propagation losses in the 1.5- to 1.58- μm spectral region are as low as 1.8 and 4.9 dB/mm for transverse-electric- and transverse-magnetic-polarization, respectively. The losses are attributed to the sidewall roughness and can be further reduced by the optimization of the etching process.

Index Terms—GaN, intersubband (ISB) devices, optical communication, optical waveguide (WG).

I. INTRODUCTION

III–NITRIDE wide bandgap semiconductor materials have attracted considerable interest in recent years for their application to blue-ultraviolet (UV) light emitters [1] and high-power high-speed electronic devices [2]. Recently, a new application field has emerged for optoelectronic devices operating at fiber-optics telecommunication wavelengths, in particular for the realization of integrated optical circuits. III–nitride based waveguides (WGs) have indeed great potential in this spectral range not only because of the material transparency but also because of the low-temperature sensitivity of their index of refraction, which is one order of magnitude smaller than that of InP. Hui *et al.* have demonstrated WG-based 2×2 directional couplers as well as 1×8 arrayed-WG gratings at $\lambda = 1.55 \mu\text{m}$ [3], [4]. Thanks to the large conduction band offset of up to 1.75 eV offered by nitride heterostructures, these materials also offer prospects for active optoelectronic devices at telecommunication wavelengths relying on intersubband (ISB) transitions [5]. All-optical switches making use of ISB absorption satura-

A. Lupu and F. H. Julien are with the Institut d'Electronique Fondamentale, UMR 8622 CNRS, University Paris Sud, 91405 Orsay, France (e-mail: anatole.lupu@ief.u-psud.fr).

S. Golka, G. Pozzovivo, and G. Strasser are with the Zentrum für Mikro-und Nanostrukturen, TU Vienna, 1040 Vienna, Austria.

E. Baumann, F. Giorgetta, and D. Hofstetter are with the University of Neuchâtel, Neuchâtel CH 2000, Switzerland.

S. Nicolay, M. Mosca, E. Feltin, J.-F. Carlin, and N. Grandjean are with the École Polytechnique Fédérale de Lausanne (EPFL), Institute of Quantum Electronics and Photonics, 1015 Lausanne, Switzerland.

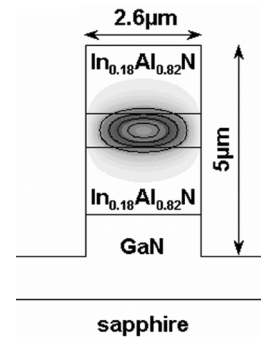


Fig. 1. WG profile and 2-D simulation of the guided TM mode (linear iso-line plot).

tion in a GaN WG have been demonstrated at $\lambda = 1.55 \mu\text{m}$ with an extinction ratio of more than 10 dB for an input pulse energy of 150 pJ [6]. The subpicosecond absorption recovery time characteristic for ISB transitions in GaN quantum wells is also of great interest for high-speed electrooptical modulators [7], [8] and photodetectors [9], [10].

So far, all III–nitride based WGs for telecommunication applications have been fabricated using GaN–AlGaIn materials grown on c-sapphire substrate either by molecular beam epitaxy or metal–organic chemical vapor deposition (MOCVD). The lattice-mismatch between GaN and AlGaIn cladding layers results in a high dislocation density, which was found to be responsible for large polarization-dependent optical losses (PDLs) [11]. In addition, the tensile strain accumulation in the AlGaIn layers prevents the growth of sufficiently thick claddings, resulting either in severe cracking or in a weak optical confinement.

In this letter, we investigate optical WGs entirely grown by MOCVD using lattice-matched materials only, namely $\text{In}_{0.18}\text{Al}_{0.82}\text{N}$ for the claddings and GaN for the WG core. We show that this original approach provides a significant reduction of PDL and propagation losses at $\lambda = 1.5 \mu\text{m}$.

II. WG DESIGN AND FABRICATION

In order to design a GaN–InAlN WG (Fig. 1) with negligible leakage of the light into the GaN buffer layer, the WG structure has been calculated with a finite-element vectorial solver. A refractive index of 2.185 for $\text{In}_{0.18}\text{Al}_{0.82}\text{N}$ and 2.335 for GaN [3], [12] was used to perform the eigenmode calculations.

For a typical sample length of a few millimeters, a WG structure with 800-nm GaN core thickness and 1.65- μm InAlN cladding layer thickness (Fig. 1) is found to be sufficient to suppress leakage towards the GaN buffer layer.

All epitaxial layers were grown in an MOVPE reactor (Aixtron 200/4 RF-S) on c-plane sapphire substrates. The bottom cladding layer was deposited on a 2- μm GaN buffer layer grown at 1075 °C. The lattice-matched InAlN was grown at a temperature of 817 °C at 75 mbar (see [12] for details). The indium content in the layer has been calibrated by X-ray diffraction measurements. The samples revealed to be crack-free with a smooth surface. The roughness is 0.9-nm root-mean-square after the growth of the lower cladding. The full-width at half-maximum of the rocking curves for the (001) reflection plane for GaN template and InAlN WG material is 281 and 285 arcsec, respectively. The dislocation density, as estimated from atomic force microscope images, is around a few 10^8 cm^{-2} which is comparable to the density present in the GaN template.

The WGs were first etched using an intermediate SiN_x mask with 900-nm thickness. A thin, sputtered Al layer had been used to block UV transmission through the substrate and enhance resist contrast. AZ5214 photoresist was spray-coated resulting in a resist thickness of $\sim 2.2 \mu\text{m}$. Al is readily etched by the developer AZ351B. The pattern was then transferred into SiN_x by SF_6 reactive ion etching (RIE) and from there into the GaN–InAlN with inductively coupled plasma (ICP)-RIE (Oxford Plasmalab100 with 65-mm ICP source). Although the nitrides are chemically inert, the use of a high plasma density at low bias allowed us to efficiently etch the nitride layers without introducing too many additional defects [13]. The high In and Al contents required heating up to 300 °C during ICP-RIE. A N_2 – SiCl_4 gas mixture (20/10 sccm, respectively) was used at a medium ICP power (120 W) and low capacitively coupled plasma power 40 W (~ 200 -V bias). The chamber pressure during this process was 5-mTorr. The selectivity with respect to SiN_x of this optimized etch recipe is ten (GaN), eight (InAlN), and five (pure AlN). WG bars of different length were fabricated by an automatic dicing saw (Disco DAD3220) with Ni bonded diamond blades.

III. PROPAGATION LOSS MEASUREMENTS

Measurements were performed with an end-fire coupling setup using a super-luminescent light-emitting diode (SLED) centered at 1550 nm with 40-nm spectral half-width and an optical spectrum analyzer (OSA). Via a polarization controller, the SLED light is coupled into the GaN WG using a polarization-maintaining lensed-fiber (see the inset in Fig. 2). The output light is collected by a 40 \times infrared (IR) objective and is either imaged onto an IR vidicon camera, a Ge diode or coupled into a single-mode fiber via a second objective, and sent into the OSA.

As in any dielectric WG, the propagation losses can be either related to the material absorption or to sidewall roughness-induced light scattering. In order to distinguish between these two different loss mechanisms, propagation loss measurements were performed on a series of various length WG with 2.6- and 60- μm -wide straight stripes. Measurements were

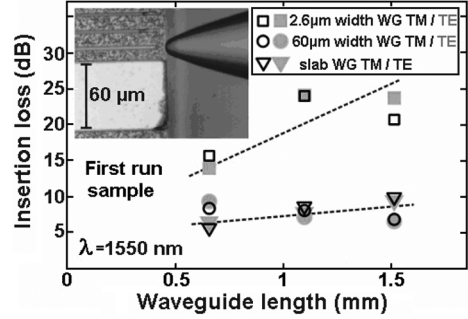


Fig. 2. Insertion loss of WGs with diced facets. Black = TM, gray = TE in all figures. Inset: fiber taper in front of diced facet.

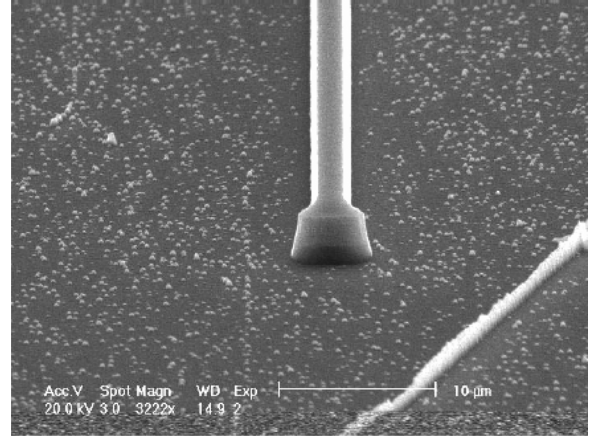


Fig. 3. SEM view of ICP-defined WG facet.

also carried out on slab WGs, i.e., without lateral confinement and sidewall scattering losses.

The light transmission measurements revealed that in the limit of the experimental error, the losses of 60 μm wide and slab WGs practically do not depend on the sample length, while for 2.6- μm -wide WGs, there is an obvious increase of losses with increasing sample length (Fig. 2).

The slope of the losses is different for narrow and slab WGs which gives clear evidence that the propagation losses are essentially related to the sidewall roughness and that the material absorption plays only a minor role. This is also supported by the fact that transverse-electric (TE) and transverse-magnetic (TM) polarized light losses are practically identical, i.e., PDL is negligible, especially in the slab WG case.

Some dispersion can be observed in the experimental data. This is due to spurious coupling losses because of the poor quality of input–output facets after diamond saw dicing.

In order to carry out Fabry–Pérot oscillations measurements and to accurately determine the propagation losses, a second fabrication run was performed, aiming at defining the WGs’ facets by ICP etching (Fig. 3).

Fig. 4 shows the WG transmission spectrum with Fabry–Pérot fringes as well as the propagation losses determined from the fringes contrast.

As one can see from the figure, the contrast of Fabry–Pérot fringes is much higher for TE than for TM polarization. The associated propagation losses are 5–6 dB/mm for TM and smaller

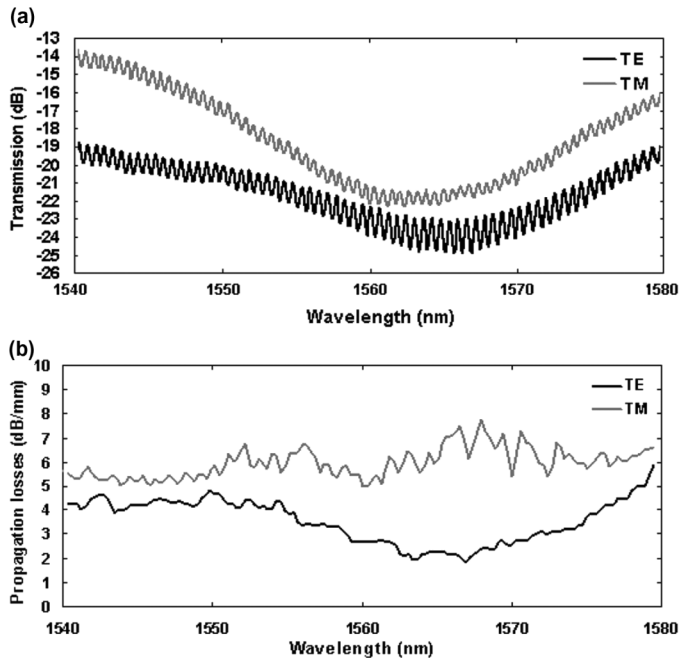


Fig. 4. (a) Normalized measured optical transmission spectrum and (b) propagation losses determined from Fabry-Pérot oscillations. TE polarization: black lines; TM polarization: gray lines in all figures.

than 4 dB/mm with a minimum of 1.8 dB/mm for TE. To the author's knowledge, these are the lowest values reported so far for the propagation losses in GaN WGs.

For loss calculations, a reflection coefficient $R = 0.147$ was assumed. This value is based on the Fresnel reflection at the semiconductor air interface. As explained above, the observed loss level is determined by the sidewall roughness. The remaining roughness present after deep etching stems from the roughness/underetch (~ 400 nm from the defined resist edge) introduced by SF_6 RIE pre patterning and not from the deep etching itself. The resulting corrugations of the WG are mainly in the propagation direction and not in the vertical direction. Due to this directionality, they might introduce PDL as well [14]; this hypothesis is consistent with higher losses for TM than for TE.

As shown in Fig. 4, the propagation losses vary as a function of the wavelength. This is probably related to WG width inhomogeneities due to technological imperfections as well as a slight multimode behavior of these WGs.

IV. SUMMARY

In conclusion, we have demonstrated the fabrication of symmetric, deeply etched GaN rib WGs. The GaN core and the lattice-matched InAlN cladding were grown by MOCVD. Transmission through slabs shows material related losses of < 3 dB/mm and negligible PDL. These results

were confirmed by propagation losses measurements on $2.6\text{-}\mu\text{m}$ -wide straight WGs. The TM/TE propagation losses extracted from Fabry-Pérot measurements are as low as $4.9 \pm 0.3/1.8 \pm 0.1$ dB/mm. These are the lowest values reported so far for GaN-based WGs. Further decrease of the propagation losses can be achieved through optimization of the WG etching process in order to reduce the sidewall roughness.

ACKNOWLEDGMENT

The authors would like to thank E. Svasek and P. Svasek for valuable support on dicing and spray-coating.

REFERENCES

- [1] S. Nakamura and G. Fasol, *The Blue Laser Diode*. Berlin: Springer, 1997.
- [2] Y. Wu, A. Saxler, M. Moore, R. P. Smith, S. Sheppard, P. M. Chavarkar, T. Wisleder, U. K. Mishra, and P. Parikh, "30-W/mm GaN HEMTs by field plate optimization," *IEEE Electron Device Lett.*, vol. 25, no. 3, pp. 117–119, Mar. 2004.
- [3] R. Hui, Y. Wan, J. Li, S. X. Jin, J. Y. Lin, and H. X. Jiang, "III-Nitride-Based planar lightwave circuits for long wavelength optical communications," *IEEE J. Quantum Electron.*, vol. 41, no. 1, pp. 100–110, Jan. 2005.
- [4] R. Hui, Y. Wan, J. Li, S. X. Jin, J. Y. Lin, and H. X. Jiang, "Birefringence of GaN/AlGaIn optical waveguides," *Appl. Phys. Lett.*, vol. 83, no. 9, pp. 1698–1700, Sep. 2003.
- [5] M. Tchernycheva, L. Nevou, L. Doyennette, F. Julien, E. Warde, F. Guillot, E. Monroy, E. Bellet-Amalric, T. Remmele, and M. Albrecht, "Systematic experimental and theoretical investigation of intersubband absorption in GaN/AlN quantum wells," *Phys. Rev. B*, vol. 73, p. 125347/10, Mar. 2006.
- [6] N. Iizuka, K. Kaneko, and N. Suzuki, "Sub-picosecond all-optical gate utilizing an intersubband transition," *Opt. Express*, vol. 13, no. 10, pp. 3835–3840, May 2005.
- [7] E. Baumann, F. R. Giorgetta, D. Hofstetter, S. Golka, W. Schrenk, G. Strasser, L. Kirste, S. Nicolay, E. Feltin, J. F. Carlin, and N. Grandjean, "Near infrared absorption and room temperature photovoltaic response in AlN/GaN superlattices grown by metal-organic vapor-phase epitaxy," *Appl. Phys. Lett.*, vol. 89, p. 041106/3, Jul. 2006.
- [8] L. Nevou, N. Kheirodin, M. Tchernycheva, L. Meignien, P. Crozat, A. Lupu, E. Warde, F. H. Julien, G. Pozzovivo, S. Golka, G. Strasser, F. Guillot, E. Monroy, T. Remmele, and M. Albrecht, "Short-wavelength intersubband electroabsorption modulation based on electron tunneling between GaN/AlN coupled quantum wells," *Appl. Phys. Lett.*, vol. 90, p. 223511/3, Jun. 2007.
- [9] D. Hofstetter, S.-S. Schad, H. Wu, W. J. Schaff, and L. F. Eastman, "GaN-AlN-based quantum-well infrared photodetector for $1.55\ \mu\text{m}$," *Appl. Phys. Lett.*, vol. 83, no. 3, pp. 572–574, Jul. 2003.
- [10] F. R. Giorgetta, E. Baumann, F. Guillot, E. Monroy, and D. Hofstetter, "High frequency $f = 2.37$ GHz room temperature operation of $1.55\ \mu\text{m}$ AlN/GaN-based intersubband detector," *Electron. Lett.*, vol. 43, no. 3, pp. 185–186, Feb. 2007.
- [11] N. Iizuka, K. Kaneko, and N. Suzuki, "Polarization dependent loss in III-nitride optical waveguides for telecommunication devices," *J. Appl. Phys.*, vol. 99, p. 0913107/3, May 2006.
- [12] J. F. Carlin, C. Zellweger, J. Dorsaz, S. Nicolay, G. Christmann, E. Feltin, R. Butté, and N. Grandjean, "Progresses in III-nitride distributed Bragg reflectors and microcavities using AlInN/GaN materials," *Phys. Stat. Sol. (b)*, vol. 242, no. 11, pp. 2326–2344, Jul. 2005.
- [13] S. J. Pearton, J. C. Zolper, R. J. Shul, and F. Ren, "GaN: Processing, defects, and devices," *J. Appl. Phys.*, vol. 86, no. 1, pp. 1–78, Jul. 1999.
- [14] M. Elson, "Propagation in planar waveguides and the effects of wall roughness," *Opt. Express*, vol. 9, no. 9, pp. 461–475, Oct. 2001.